Excess silicon at the silicon nitride/thermal oxide interface in oxide–nitride–oxide structures

V. A. Gritsenko[a)]
Institute of Semiconductor Physics, Novosibirsk 630090, Russia

Hei Wong
Department of Electronic Engineering, Cityu, 83 Tat Chee Avenue, Kowloon, Hong Kong

J. B. Xu and R. M. Kwok
Chinese University of Hong Kong, Shatin, Hong Kong

I. P. Petrenko and B. A. Zaitsev
Institute of Semiconductor Physics, Novosibirsk 630090, Russia

Yu. N. Morokov
Institute of Computational Technologies, Novosibirsk 630090, Russia

Yu. N. Novikov
Institute of Semiconductor Physics, Novosibirsk 630090, Russia

(Received 15 September 1998; accepted for publication 9 June 1999)

The chemical composition and structure of Si_3N_4/thermal (native and wet) SiO_2 interface in oxide–nitride–oxide structures are studied by using secondary ion mass spectroscopy, electron energy loss spectroscopy (EELS) and Auger electron spectroscopy (AES) measurements. EELS and AES experiments show the existence of excess silicon at the Si_3N_4/thermal SiO_2 interface. Excess silicon (Si–Si bonds) at Si_3N_4/SiO_2 interface exists in the form of Si-rich silicon oxynitride. Numerical simulation of the Si–Si bond's electronic structure by using semiempirical quantum-chemical method (MINDO/3) shows that Si–Si defects act as either electron or hole traps. This result explains the abnormally large electron and hole capturing at this interface reported earlier. © *1999 American Institute of Physics.* [S0021-8979(99)03418-0]

I. INTRODUCTION

Oxide–nitride–oxide (ONO) structure has been widely used as dielectric in the dynamic random access memory (DRAM) and electrically erasable programmable read only memory (EEPROM) devices. The ONO structure is also used as interpoly dielectric for multilevel metallization in complementary metal–oxide–semiconductor (CMOS) technology.[1,2] In comparison to thermal oxide, the ONO structure has lower leakage current, higher effective dielectric permittivity, and higher reliability. Electron capturing on the traps in Si_3N_4, which reduces barrier at the negatively biased electrode interface, gives rise to the low leakage current. Although anomalous large trapping of electrons at the Si_3N_4/thermal SiO_2 interface in the silicon–oxide–nitride–oxide–silicon (SONOS) EEPROM is often reported experimentally,[3–5] the nature of electron and hole capturing in the ONO structure is still unclear. This work aims to study the excess silicon at the Si_3N_4/thermal SiO_2 interface by using secondary ion mass spectroscopy (SIMS), electron energy loss spectroscopy (EELS), and Auger electron spectroscopy (AES) measurements. To understand the nature of electron and hole traps at this interface, numerical simulation of the electronic structure of Si–Si is also performed. Some preliminary results obtained by EELS and ellipsometry have been published.[6] A more complete and systematic investigation of the excess silicon at the Si_3N_4/thermal SiO_2 interface was conducted in this work. The experimental details are given in Sec. II. Section III presents the experimental results obtained from SIMS, EELS, and AES measurements. Based on the measurement results, in Sec. IV, we propose a model to explain the creation of Si–Si bonds at the oxide/nitride interface and the phenomenon of nitrogen dissipation during the oxide nitridation. Section V presents the numerical simulation results of the trapping properties of Si–Si bonds in oxide and nitrides and further discussions on these topics will be given in Sec. VI. Finally, major results of this work will be summarized in Sec. VII.

II. SAMPLE PREPARATION AND MEASUREMENT

Samples with silicon–oxide–nitride–thermal–oxide (SONO) structure were fabricated on *p*-type silicon with ⟨100⟩ or ⟨111⟩ orientation and the resistivity is about 10 Ω cm. A thin thermal oxide of 18 or 60 Å was first grown with dry oxidation, and then a low-pressure chemical vapor deposition (LPCVD) Si_3N_4 was deposited on the thermal oxide at 800 °C using $SiCl_4$ and NH_3 mixture. Thickness of Si_3N_4 film was 400 Å for SIMS measurements and about 150 Å for EELS and AES measurements to minimize the charging effects. Thermal oxide on Si_3N_4 was either ''native'' or produced by wet oxidation. Native oxide was

a)Gritsenko was visiting scholar of Chinese University of Hong Kong. Electronic mail: vladimir@isp.nsc.ru

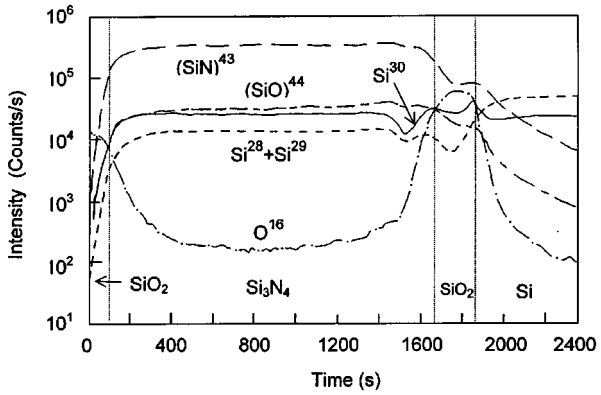

FIG. 1. SIMS depth profile of Si/SiO_2 (60 Å)/Si_3N_4 (380 Å)/wet SiO_2 (30 Å) structure.

formed when removing the sample from the hot LPCVD reactor to room atmosphere, whereas the wet oxidation was made at 900 °C for 52 min.

For SIMS depth profiling, Riber MIQ156 SIMS instrument was used. The beam source is 5 keV Cs^+ and the beam current is 50 nA. EELS and AES measurements were made with Riber model LAS-3000 Auger electron spectrometer. The electron beam with energy in the range of 100–3000 eV, with 90° incident angle, was used and the reflected electrons were measured at 42° with a cylinder mirror analyzer.

III. EXPERIMENTAL RESULTS

A. SIMS measurements

To verify the existence of excess silicon at the Si_3N_4/SiO_2 interface in SONO structures, SIMS measurement was conducted. Figure 1 depicts the SIMS depth profile of the structure with wet top oxide. Vertical lines show the interface positions. To observe the Si–Si bonds at Si_3N_4/wet SiO_2 interface, mass spectra of species with mass 57 ($Si^{28}+Si^{29}$) were detected. No Si–Si signal at Si_3N_4/wet SiO_2 interface can be observed. However, a notable mass 57 peak was found at the nitride/bottom oxide interface. The absence of mass 57 peak at top oxide/nitride interface may be due to the poor resolution of SIMS measurement as the interface layer is so thin. In addition, significant recoil or radiation enhanced diffusion[7] effects may also give rise to the inaccuracy of the measurement. As shown in the figure, remarkable N and O tails are found in the Si substrate. Since the Cs^+ ion energy (5 keV) used for sputtering is much larger than that of bonding energy (3–5 eV) of Si–Si bond, the Cs^+ ions broke the Si–O, Si–N, Si–Si, and other bonds. The ionized atoms may be recombined or redistributed.[7] Thus, the SIMS spectra may not reflect the real distribution of atoms and bonds in the sample. With this connection, further investigation on the physical structure of the sample was conducted by using other kinds of analytical tools.

B. Electron energy loss spectroscopy

Electron energy loss spectroscopy involves measuring the plasmon energy of the valence electron oscillation. In the free electron approximation, the bulk plasmon energy ($\hbar\omega_B$) is governed by the density of valence electron (N_v) and is given by

$$(\hbar\omega_B)^2 = 4\pi\hbar^2 e^2 N_V / m^*, \tag{1}$$

where m^* is the electron effective mass, and the density of valence electron is governed by

$$N_V = N_A \rho \frac{n_{\mathrm{Si}} + \frac{4}{3} n_{\mathrm{N}}}{A_{\mathrm{Si}} + \frac{4}{3} A_{\mathrm{N}}}, \tag{2}$$

where ρ is the Si_3N_4 atomic density, N_A is the Avogadro number, A_{Si} and A_{N} are the atomic weights of silicon and nitrogen, respectively, and n_{Si} and n_{N} are the numbers of valence electrons per silicon and per nitrogen atom taking part in the plasmon oscillation, respectively.

Since the densities of valance electrons (N_v) in Si_3N_4, SiO_2, and Si are different, the bulk plasmon energies in these materials will be also different. On the other hand, it is well known that the electron escape depth (EED) in solid is also governed by the electron energy. For instance, at the excitation energy of 1486.6 eV, the Si 2*p* electrons with kinetic energy of about 1380 eV (about 100 eV lower than the excitation energy) have an EED of 21.1 Å in Si and 29.6 Å in SiO_2.[8] The same Si 2*p* electrons at the excitation energy 130 eV (or kinetic energy of about 30 eV) have an EED of only 4 Å in Si and 7 Å in SiO_2.[9] The EED value can be reduced by decreasing the electron beam energy in the range of 100 to 1000 eV. Hence, the bulk plasmons can be studied with high-energy EELS and the thin layer properties can be studied by using low-energy EELS.

It is well known that the bulk plasmon energies ($\hbar\omega_B$), determined from x-ray photoelectron spectroscopy (XPS) loss spectra, for Si_3N_4, SiO_2, and Si are 24.0 eV (from N 1*s* level), 23.0 eV (from O 1*s*), and 17.0 eV (from Si 2*p*), respectively. The accuracy of this measurement is about 1 eV. More accurate (about 0.3 eV) values of bulk plasmon energies were obtained by using high energy (3000 eV) EELS. The results are depicted in Fig. 2. As shown in Fig. 2, values of plasmon energies are the same as those obtained from XPS measurements. In addition, multiple plasmon excitations (three plasmons in Si and two plasmons in SiO_2 and Si_3N_4) were observed which are indicated by arrows in Fig. 2. No surface plasmons with energy $\hbar\omega_B/\sqrt{2}$ were found. The 24.0 eV plasmon for Si_3N_4 corresponds to $n_{\mathrm{Si}}=4$ and $n_N=5$ at the Si_3N_4 density $\rho=3.0$ g/cm^3.[10] Parameter $n_{\mathrm{N}}=5$ is a result of the plasmon oscillation of (a) Si 3*s*, 3*p*, N 2*p* bonding; (b) N $2p_\pi$ nonbonding nitrogen electrons of top valence band; and (c) two N 2*s* electrons of lower valence band.[11] This result is different from the conclusion drawn by Guraya *et al.*[12] who reported $n_{\mathrm{N}}=3$, which corresponds to the plasmon oscillation from three *p* nitrogen electrons of top valence band of Si_3N_4.

To study the Si_3N_4/SiO_2 interface by EELS, the oxide on Si_3N_4 was etched in $HF:H_2O=1:30$ solution. The etching rate of SiO_2 in this solution is about 1 Å/s (estimated by using XPS measurement). After the thermal oxide was removed, EELS measurement with different electron beam energy was conducted on the Si_3N_4 surface. As shown in Fig.

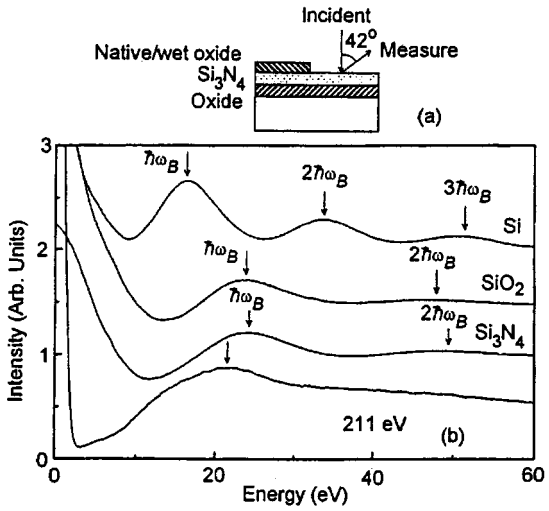

FIG. 2. (a) Illustration of sample structure, incident angle of beam source, and angle for measuring reflected electrons. (b) EELS spectra of bulk Si, SiO_2, and Si_3N_4 at electron beam energy of 3000 eV, and low-energy (211 eV) EELS of Si_3N_4/wet SiO_2 structure after the removal of top SiO_2.

3, decrease of electron beam energy for EELS measurement gives rise to a low-energy shift and widening of the plasmon peak. A plasmon peak at energy of about 20 eV and with a large width was found at electron beam energy of 100 eV at Si_3N_4/native SiO_2 interface. Same results were obtained for Si_3N_4/wet SiO_2 interface. As shown in Fig. 2, at low electron beam energy (211 eV) wide plasmon peak with energy about 21–22 eV for Si_3N_4/wet SiO_2 interface is observed. These observations indicate the existence of excess silicon at Si_3N_4/oxide interface.

Figure 4 shows the second derivative of EELS measured on Si_3N_4 after the surface native and wet SiO_2 were removed. The high-energy peaks with energy 20.3 and 21.1 eV can be seen clearly for structures with native and wet oxide, respectively. These peaks are attributed to the plasmon oscillation of transitional layer at Si_3N_4/SiO_2 interface. The low-energy peaks are probably due to the defect excitations or/and interband transitions.

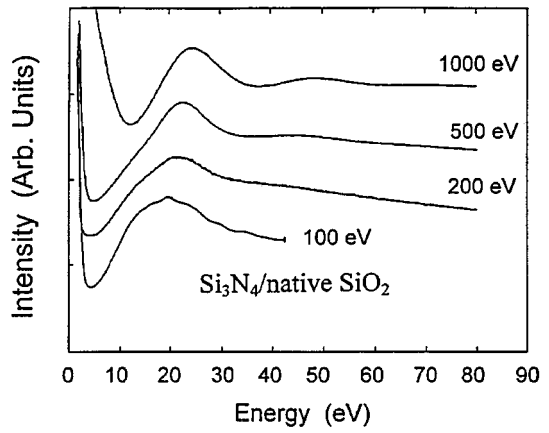

FIG. 3. EELS of Si_3N_4/native SiO_2 interface after the removal of the native SiO_2 taken at different electron beam energies.

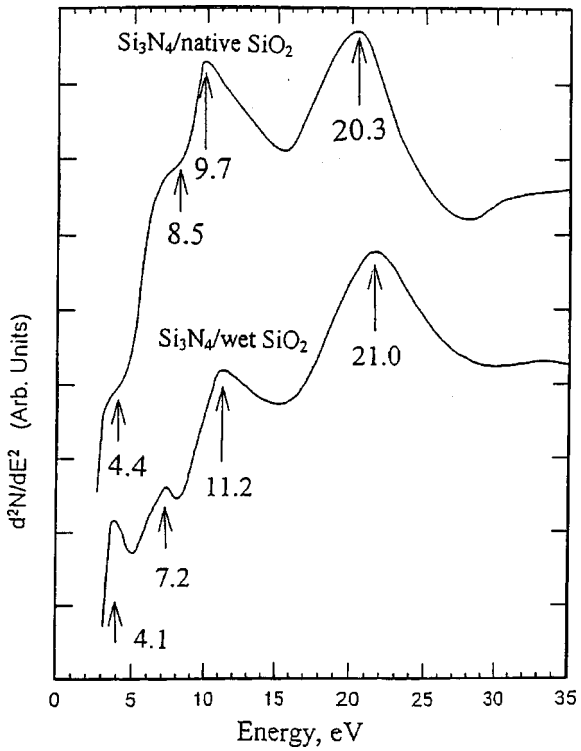

FIG. 4. Second derivative of EELS of Si_3N_4/native SiO_2 and Si_3N_4/wet SiO_2 structures measured at 200 eV electron beam energy after the removal of top oxide layer.

It is noted that the second derivative EELS is very sensitive to the etching time and the measurement conditions (electron beam energy and current). All measurement shows a common result that the plasmon losses at Si_3N_4/native, wet SiO_2 interface have energy in the range of 20–22 eV. The obtained plasmon energies of transitional layer at Si_3N_4/native, and wet SiO_2 interface are lower than those of bulk Si_3N_4 and SiO_2. Plasmon with energy 19.6 eV at the Si_3N_4/native oxide interface was obtained by Hezel and Lieske.[13] By lowering the electron beam energy from 2500 to 100 eV, Lifshiz *et al.*[14] also found that the plasmon energy of Si_3N_4 with native oxide decreases from 24 to 20 eV. However, no explanation for these low plasmon energies was proposed in their papers.

To sum up, we have found that the decrease of the electron beam energy from 1000 to 100 eV gives rise to the decrease of the plasmon energy and the increase of its width at the Si_3N_4/native and Si_3N_4/wet oxide interfaces. These observations can be explained as follows. A reduction in the electron energy will result in the decrease of the EED. Then, the surface components that have lower plasmon energy appear as a result. First-order approximation can be made by assuming the low energy plasmon peak at 100 eV is composed of two peaks corresponding to Si_3N_4 and Si. Since the EED in SiO_2 measured at energy of 70 eV is about 6.6 Å,[15] and the effective width of ''silicon-rich'' interfacial layer, roughly equal to the EED, in SiO_2 is in the range of 6–8 Å which is consistent with the value estimated by Lifshiz *et al.*[14]

For nonstoichiometric silicon nitride $SiN_{x<4/3}$ (enriched with excess silicon), its plasmon energy decreases from 22 to

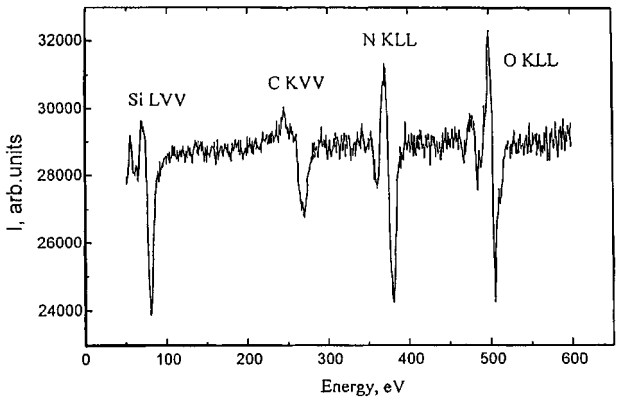

FIG. 5. Survey of AES spectra of the Si_3N_4/wet SiO_2 interface after the top SiO_2 being etched away.

17 eV.[12,16] Quantitatively, the relation between the valence electron density and silicon concentration in SiN_x is governed by

$$N_V = \rho \frac{n_{\mathrm{Si}} + x n_{\mathrm{N}}}{A_{\mathrm{Si}} + x A_{\mathrm{N}}} N_A, \tag{3}$$

where ρ is the a-SiN_x atomic density, and x (=N/Si) indicates the a-SiN_x chemical composition. The atomic density of SiN_x decreases from $\rho = 3.0$ g/cm^3 for Si_3N_4 to 2.33 g/cm^3 for Si. Equations (3) and (1) together explain the decrease of plasmon energy ($\hbar\omega_B$) by increasing of excess silicon concentration.

Similarly, enriching of $SiO_{x<2}$ with excess silicon would also lead to the decrease of plasmon energy.[17] The decrease of plasmon energy in SiN_x and SiO_x in Si-rich dielectrics is due to high Si–Si bond concentration. So, the transitional layer at Si_3N_4/SiO_2 interface should be Si-rich silicon oxynitride. When the silicon oxynitride (SiO_xN_y) is grown at excess oxygen and nitrogen ambient, it consists of Si–O and Si–N bonds only.[18] In such SiO_xN_y film, each Si atom is coordinated with four O and/or N atoms, each N atom coordinated with three Si atoms, and each O atom is coordinated with two Si atoms.[19] The SiO_xN_y without Si–Si bonds consists of five sort of tetrahedrons $SiO_\nu N_{4-\nu}$, $\nu = 0, 1, 2, 3, 4$. The physical properties of SiO_xN_y without Si–Si bonds change gradually from those of SiO_2 to Si_3N_4 as the nitrogen concentration increases and oxide concentration decreases.[20,21] In this case, the plasmon energy of SiO_xN_y must be between 22.0 and 24.0 eV. However, in our experiment the plasmon energy at the Si_3N_4/SiO_2 interface is in the range of 20–22 eV. We thus propose that the SiO_xN_y at the interface is Si-rich and consists of Si–O, Si–N and Si–Si bonds. AES measurements were conducted to verify this hypothesis.

C. Auger spectroscopy

Figure 5 displays the survey of AES spectrum of Si_3N_4/wet SiO_2 interface after the top oxide is removed. Following AES transition energies were registered: N *KLL* (381.5 eV), O *KLL* (505.5 eV), C *KLL* (271.0 eV), and Si *LVV* (86.0 eV). The Si *LVV* energy measured at the Si_3N_4/wet SiO_2 interface has an energy of 86.0 eV which is

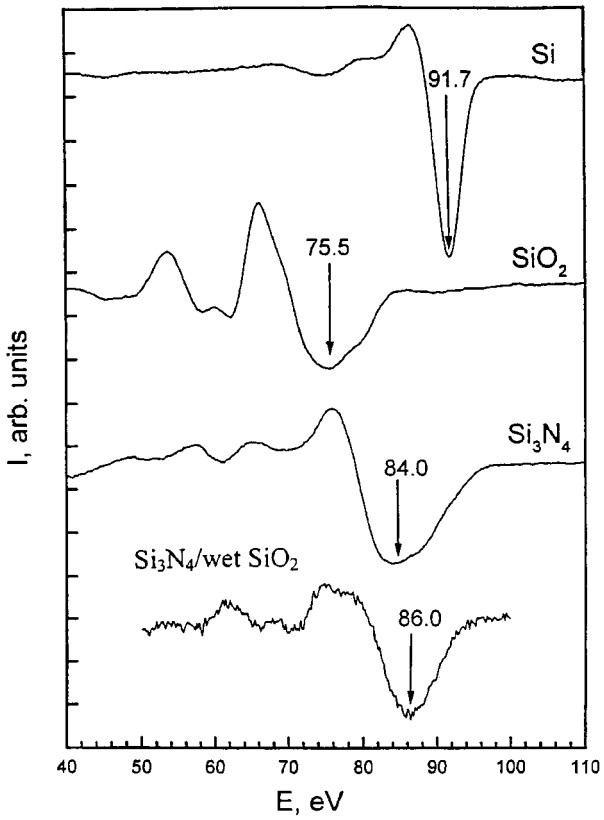

FIG. 6. Si *LVV* AES spectrum of the Si, SiO_2, and Si_3N_4 bulk, and Si_3N_4/wet SiO_2 interface after the removal of top oxide.

higher than that of SiO_2 (75.5 eV) and Si_3N_4 (84.0 eV) but lower than that of Si (91.7 eV). This result strongly suggested that Si–Si bonds exist in the transitional layer at Si_3N_4/wet SiO_2 interface. Since the survey of AES spectra (Fig. 5) shows the existence of both oxygen and nitrogen at Si_3N_4/SiO_2 interface, we propose that the transition layer at the Si_3N_4/SiO_2 interface is Si-rich SiO_xN_y. The effective thickness of Si-rich SiO_xN_y layer is in the same order of Si *LVV* electron escape depth (6–8 Å). This value is in agreement with the value estimated by using EELS.[14] Figure 6 shows the Si AES spectra of Si, and Si_3N_4 and SiO_2. The kinetic energies of Si *LVV* transition in Si, Si_3N_4, and SiO_2 are of 91.7, 84.0, and 75.5 eV, respectively. The chemical shift of Si *LVV* signal in Si, Si_3N_4, and SiO_2 gives qualitative information on the coordination conditions of silicon atoms. The escape depth of Si *LVV* electrons is in the range of 6–8 Å. Hence AES measurements is also a good tool to verify the existence of Si–Si bonds at the Si_3N_4/SiO_2 interface.

It can be estimated that the silicon atom densities in SiO_2, Si_3N_4 and Si are 2.2×10^{22}, 3.9×10^{22}, and 5.0×10^{22} cm^{-3}, respectively. If the density of excess silicon in the transitional interface layer at the Si_3N_4/thermal SiO_2 interface is close to that of Si, then the excess silicon can be found directly using AES or SIMS profiling. Figure 7 shows the depth profile of the AES peak intensities for the Si/SiO_2 (60 Å)/Si_3N_4 (380 Å)/wet SiO_2 (30 Å) (SONO) structure. Here, the Ar^+ ion beam energy is 5 keV. The etching time of top oxide on Si_3N_4 is about 2 min. As shown in Fig. 7, the

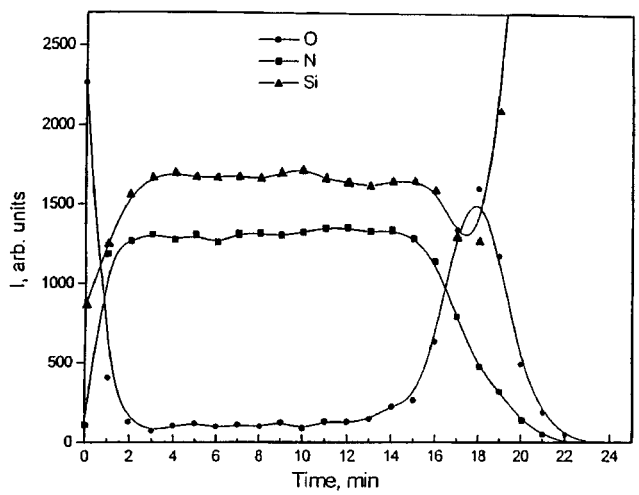

FIG. 7. Depth profile of the AES peak intensities for the Si/SiO_2 (60 Å)/ Si_3N_4 (380 Å/wet SiO_2 (30 Å) structure.

existence of oxygen in bottom and top oxide in SONO structure is clear. However, similar to the results reported by Chao *et al.*,[22] no excess silicon at Si_3N_4/wet SiO_2 interface was observed. It was shown that the Ar^+ etching of SiO_2 and Si_3N_4 could result in the enriching of bombarded surface layer with excess silicon and produce artifacts.[23] This is probably the main reason that the AES profile does not have excess silicon at Si_3N_4/thermal SiO_2 interface. Nevertheless, our Si *LVV* AES measurements do show the existence of Si–Si bonds in the Si-rich SiO_xN_y layer at the Si_3N_4/wet SiO_2 interface.

IV. MECHANISM OF SI–SI BOND CREATION

The existence of Si–Si bond at the interface has been confirmed with EELS and AES measurements. The Si–Si bonds are formed by the substitution of the nitrogen atoms by the oxygen atoms.[24,25] Since an N atom in Si_3N_4 is coordinated by three Si atoms, and an O atom in SiO_2 is coordinated by two Si atoms,[17,19] substitution of N by O is described in the following reaction:

$$2{\equiv}Si_3N+2O\rightarrow 2{\equiv}Si_2O+2{\equiv}Si\cdot+2N$$
$${\equiv}Si\cdot+\cdot Si{\equiv}\rightarrow{\equiv}Si-Si{\equiv}. \quad (4)$$

The creation of Si–Si bonds during reoxidation of SiO_xN_y results from the replacement of N-atoms with O-atoms (with lower coordination number).[25] The $\equiv Si_3N$ species are also found in the top surface region of SiO_xN_y during SiO_2 nitridation.[8] Reoxidation of SiO_xN_y results in the replacing of nitrogen atoms by oxygen atoms according to Eq. (4). Si–Si bonds should also be formed at the SiO_xN_y/SiO_2 interface. This conjecture is supported by the experiment conducted by Yount *et al.*[26] It was shown that at the top surface of reoxidized SiO_xN_y there is a high density of E' centers which are Si–Si bonds with hole trapping.

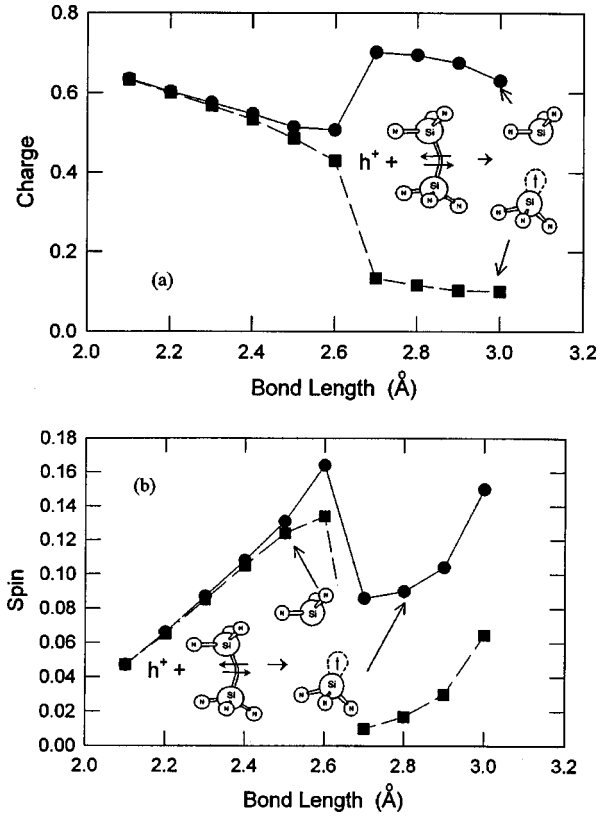

FIG. 8. (a) Charge and (b) spin variations of silicon atom pair for the Si–Si bond with a captured hole ($q=+1$) in Si_3N_4 at different Si–Si distances. The inserts show the spin distribution of silicon atoms.

V. NUMERICAL SIMULATION OF SI–SI BOND CAPTURING PROPERTIES

Qualitative polaron model for the multiphonon electron and hole capturing in the neutral Si–Si bond in Si_3N_4 was proposed and developed.[19,21,24,27–29] Numerical simulation of the Si–Si bonds electronic structure in Si_3N_4 and SiO_2 was conducted in the present work by the semiempirical quantum-chemical method (MINDO/3) where atomic relaxation after electron or hole localization was considered. Two minimal clusters $H_6N_3Si–SiN_3H_6$ and $H_3O_3Si–SiO_3H_3$ were used to simulate the Si–Si bond in Si_3N_4 and SiO_2, respectively. The dangling bonds of the boundary atoms are passivated with hydrogen atoms. The values of the empirical parameters α and β, describing the bonds of coupling atoms for the Si–N bonds, were determined by reproducing the experimental partial density of states in Si_3N_4.[13] The obtained values are: $\alpha=1.053011$ and $\beta=0.434749$.

Figure 8 displays the charge and spin distributions of two central silicon atoms with positively charged Si–Si bond (when a hole is localized on Si–Si defect) as a function of initial Si–Si bond separation. Symmetric atom relaxation and symmetric distribution of the electron density for small initial Si–Si separations are found. As the initial Si-Si separation increases, the atomic relaxation becomes asymmetric. At a distance larger than 2.6 Å, asymmetric relaxation of the silicon atoms is observed. The positively charged silicon atom moves to the plane direction of three nitrogen atoms whereas the neutral silicon atom (with unpaired electron)

TABLE I. Electron and hole delocalization energies in Si–Si bond in Si_3N_4 calculated using Koopman theorem.

Bond/defect	Electron delocalization energy (eV)	Hole delocalization energy (eV)
$d_{Si-Si}=2.3$ Å	0.3540	0.1956
$d_{Si-Si}=3.0$ Å	0.8138	0.2922

moves away from the nitrogen atoms. This situation is similar to the E' center in SiO_2, which is a Si–Si neutral bond with a captured hole. Capturing of hole on a Si–Si bond in Si_3N_4 accompanies the spin polarization and is an active defect in electron spin resonance (ESR) measurement.[29] The silicon atom with an unpaired electron coordinated with three nitrogen atoms ($N_3Si\cdot$) is the well-known paramagnetic K center in Si_3N_4 with $g=2.003$.[30]

A similar simulation of the Si–Si bond in Si_3N_4 with captured electron was also conducted. For Si–Si distance between 2.2 and 4.0 Å, the capturing of electron accompanies a symmetric Si–Si bond relaxation, and both silicon atoms shift to the nitrogen-atom side. The charge and spin distributions for both silicon atoms are symmetric in that case. In addition, only those Si–Si bonds with a distance larger than 4.0 Å have spin and charge polarization.

The delocalization energies of electrons and holes were calculated using the total cluster energies estimated from Koopman's theorem. The energy for hole (E^h) and electron (E^e) delocalization from Si–Si bond can be approximated by Eqs. (5) and (6), respectively.

$$E^h=(E_d^0+E_b^+)-(E_d^++E_b^0), \tag{5}$$

$$E^e=(E_d^0+E_b^-)-(E_d^-+E_b^0), \tag{6}$$

where E_b and E_d are the total energies of bulk Si_3N_4 and $H_6N_3Si–SiN_3H_6$ cluster which has been used for simulating the Si–Si defect in Si_3N_4. The upper h and e indices represent hole and electron being captured in the cluster, respectively. U84 clusters with chemical formula $Si_{20}N_{28}H_{36}$ was used for simulating the bulk properties of Si_3N_4. The U84 cluster contains 64 Si–N bonds, 6 Si–H bonds, 5 Si_2–H bonds, 18 N–H bonds and 1 N_2–H bond. Table I lists the electron and hole delocalization energies, calculated using Eqs. (5) and (6) for two Si–Si distances. The Si–Si distance of 2.3 Å is close to the distance between silicon atoms in crystalline and amorphous silicon (2.35 Å). The value 3.0 Å is close to the distance between silicon atoms in Si_3N_4. This simulation shows that the Si–Si bonds in Si_3N_4 can capture both holes and electrons. Figure 9 displays the model of electron and hole capturing on the Si–Si defect in Si_3N_4.

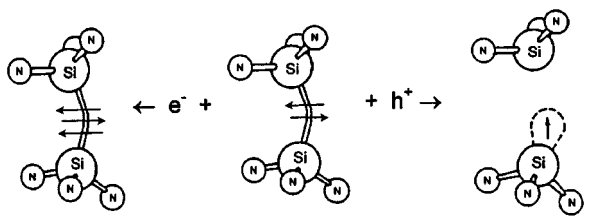

FIG. 9. Atomic model of amphoteric neutral diamagnetic Si–Si defect with electron and hole capturing in Si_3N_4.

Similar simulation was made for $H_3O_3Si–SiO_3H_3$ cluster which simulates the Si–Si bond in SiO_2 film. It was obtained that the Si–Si bonds in SiO_2 can capture both holes and electrons.[31–34] The Si–Si bond coordinated only with N atoms or only with O atoms are two extreme cases of Si-rich SiO_xN_y. More generally, the Si–Si bond in SiO_xN_y is coordinated with both O and N atoms, and it is reasonable to anticipate that Si–Si bonds in Si-rich SiO_xN_y can be both electron and hole traps.

VI. DISCUSSION

Direct evidence of existence of excess silicon at Si_3N_4/native SiO_2 interface in ONO structures had been found by quantitative analysis using XPS combined with high resolution chemical etching[35] and spectroscopic ellipsometric measurements.[36] The Si *LVV* AES experiment in the present work shows that Si–Si bonds exist at the Si_3N_4/thermal SiO_2 interface in the form of Si-rich SiO_xN_y. Since the Si–Si bonds in Si_3N_4 and in SiO_2 can capture both electrons and holes, we propose that the Si–Si bonds at the Si_3N_4/SiO_2 interface are the responsible candidates for the abnormally large electron and hole capturing in the ONO structures.[3–5]

On the other hand, it was found that nitrogen atoms dissipated at the Si_3N_4/SiO_2 interface during annealing of silicon oxide in NH_3 at 900 °C.[36] However, no explanation of this effect was proposed. Based on the fact that Si–Si bonds exist at the Si_3N_4/SiO_2 interface, we propose that the dissipation of nitrogen is due to the following reaction:

$$3{\equiv}Si–Si+2N\rightarrow 2{\equiv}Si_3N. \tag{7}$$

Reaction (7) also explains the removal of Si–Si bonds at the Si/SiO_2 interface after SiO_2 nitridation.[24,25]

It is well known that after SiO_2 nitridation $\equiv Si_3N$ species are found in the top surface region of SiO_xN_y.[37] Reoxidation results in the growth of SiO_2 on SiO_xN_y surface. It was shown in the top surface region of the reoxidized SiO_xN_y that high density of E' center was found.[8] E' center is created after a hole is captured on the Si–Si bond in the SiO_2 according to the following reaction:

$${\equiv}Si–Si{\equiv}+h\rightarrow{\equiv}Si^+ + \cdot Si{\equiv}. \tag{8}$$

In Sec. V, it was shown that the Si–Si bonds could be both hole and electron traps. It is reasonable to propose that the Si–Si bonds at the SiO_xN_y/thermal SiO_2 interface are created by nitrogen atom replacement according to reaction (4). The hole traps (Si–Si bonds) in top surface region of the reoxidized nitrided oxide can be created with the mechanism similar to the creation of Si–Si bonds during Si_3N_4 oxidation.

It is clear that the oxidation mechanism of Si_3N_4 shall be more complicated than that proposed merely based on the transformation of Si–N bonds into Si–O bonds. In fact, some abnormal kinetic of Si_3N_4 oxidation were found.[38] Si–Si bond creation during the Si_3N_4 oxidation could be one of the regimes for the observed abnormal kinetic.

VII. CONCLUSION

This comparative study shows that the excess silicon at the nitride/oxide interface cannot be detected from SIMS or AES profiling as the amount of excess silicon could be very low and the techniques used may also produce artifacts. However, excess silicon, in the form of Si–Si bond, does exist at Si_3N_4/oxide interface as evidenced by the EELS, Si *LVV* AES measurements. Interface excess silicon has profound effects on electrical properties of the dielectric film and its trapping properties have been studied using MINDO/3 simulation in this work. The main results are:

(1) The EELS and Si *LVV* AES results show the existence of Si-rich SiO_xN_y layer at the Si_3N_4/SiO_2 interface. The estimated width of this layer is in the range of 6–8 Å.

(2) The Si–Si bond creation at the Si_3N_4/thermal SiO_2 during Si_3N_4 oxidation is explained with the replacement of threefold coordinated N-atom by twofold coordinated O atom.

(3) Numerical simulation of Si–Si bond in Si_3N_4 and SiO_2 shows that the Si–Si defect can capture both electron and hole. This result explains the abnormally large electron and hole trapping at Si_3N_4/thermal SiO_2 interface observed earlier.

(4) The Si–Si bond in reoxidized nitrided oxide explains the positive charge accumulation in the top surface region of reoxidized nitrided oxide during ionizing radiation and hot-hole injection.

[1] P. C. Fazan, A. Ditali, C. H. Dennison, H. E. Rhodes, H. C. Chan, and Y. C. Liu, J. Electrochem. Soc. **138**, 2052 (1991).
[2] S. Minami and Y. Kamigaki, IEEE Trans. Electron Devices **40**, 2011 (1993).
[3] E. Suzuki, Y. Hayashi, K. Ishi, and T. Tsuchiya, Appl. Phys. Lett. **42**, 608 (1983).
[4] A. P. Aganin, V. M. Maslovskii, and A. P. Nagin, Microelectronics **17**, 348 (1988).
[5] Z. A. Weinberg, K. J. Stein, T. N. Nguen, and J. Y. Sun, Appl. Phys. Lett. **57**, 1248 (1990).
[6] V. A. Gritsenko, I. P. Petrenko, S. N. Svitasheva, and H. Wong, Appl. Phys. Lett. **72**, 462 (1998).
[7] I. Banerjee and D. Kuzminov, Appl. Phys. Lett. **62**, 1541 (1993).
[8] Z. H. Lu, J. P. McCaffrey, B. Brar, G. D. Willk, R. M. Wallace, L. C. Feldman, and S. P. Tay, Appl. Phys. Lett. **71**, 2764 (1997).
[9] F. Rochet, C. Poncey, G. Dutour, H. Roulet, C. Guillot, and F. Sirotti, J. Non-Cryst. Solids **216**, 148 (1997).
[10] V. P. Bolotin, I. A. Brytov, V. A. Gritsenko, B. Z. Olshanezkii, V. P. Popov, Yu. N. Romashenko, V. G. Serapin, and S. A. Tiis, Sov. Phys. Dokl. **310**, 114 (1990).
[11] V. A. Gritsenko, Yu. N. Morokov, and Yu. N. Novikov, Solid State Phys. **39**, 1191 (1997).
[12] M. M. Guraya, H. Ascolani, G. Zampiery, J. I. Cisneros, J. H. Diasda Silva, and M. P. Cantao, Phys. Rev. B **49**, 5677 (1990).
[13] R. Hezel and N. Lieske, Inst. Phys. Conf. Ser. **50**, 206 (1980).
[14] V. G. Lifshiz, V. G. Kotlar, and A. A. Saranin, Surface (Sov) **12**, 76 (1984).
[15] J. Himpsel, F. R. McFeely, A. Tabel-Ibragimi, J. A. Yarmoff, and G. Hollinger, Phys. Rev. B **38**, 6084 (1988).
[16] R. Karcher, L. Ley, and R. L. Johnson, Phys. Rev. B **30**, 1896 (1984).
[17] F. G. Bell and L. Ley, Phys. Rev. B **37**, 8383 (1988).
[18] I. A. Brytov, V. A. Gritsenko, and Yu. N. Romashenko, Sov. Phys. JETP **89**, 321 (1985).
[19] V. A. Gritsenko, in *Silicon Nitride in Electronics* (Elsevier, New York, 1988), p. 138–187.
[20] V. A. Gritsenko, N. D. Dikovskaja, and K. P. Mogilnikov, Thin Solid Films **51**, 353 (1978).
[21] V. A. Gritsenko, *Structure and Electronic Properties of Amorphous Dielectrics in Silicon MIS Structures* (Science, Novosibirsk, Russia, 1993), p. 280.
[22] T. S. Chao, C. L. Lee, and T. F. Lei, J. Appl. Phys. **73**, 1732 (1993).
[23] R. S. Bhattarya and P. H. Holloway, Appl. Phys. Lett. **38**, 545 (1981).
[24] V. A. Gritsenko, in *Proceedings of the NATO Advanced Research Workshop: Fundamental Aspects of Ultrathin Dielectrics on Si-based Devices Toward an Atomic Scale Understanding* (Klumer Academic, Boston, 1997), p. 411–424.
[25] V. A. Gritsenko, J. B. Xu, I. H. Wilson, R. W. M. Kwok, and Y. H. Ng, Phys. Rev. Lett. **81**, 1054 (1998).
[26] J. T. Yount, P. M. Lenahan, and G. J. Dunn, IEEE Trans. Nucl. Sci. **39**, 2211 (1992).
[27] P. A. Pundur, J. G. Shavalgin, and V. A. Gritsenko, Phys. Status Solidi A **94**, K107 (1986).
[28] V. A. Gritsenko, E. E. Meerson, I. V. Travkov, and Yu. V. Goltvjanskii, Microelectronics **16**, 42 (1987).
[29] V. A. Gritsenko and A. D. Milov, JETP Lett. **64**, 531 (1996).
[30] W. L. Warren and P. M. Lenahan, Phys. Rev. B **42**, 1773 (1990).
[31] V. O. Sokolov and V. B. Sulimov, Phys. Status Solidi B **135**, 369 (1986).
[32] J. K. Rudra and W. B. Fowler, Phys. Rev. B **35**, 8223 (1987).
[33] V. A. Gritsenko, Yu. N. Morokov, Yu. N. Novikov, H. Wong, and Y. C. Cheng, in *Proceedings of 1996 MRS Conference*, Vol. 446: *Amorphous and Crystalline Insulating Thin Films-1996* (Klumer Academic, Boston, 1997), p. 169–173.
[34] V. A. Gritsenko, Yu. N. Novikov, Yu. N. Morokov, and H. Wong, Microelectron. Reliab. **38**, 1413 (1998).
[35] E. C. Carr and R. A. Buhrman, Appl. Phys. Lett. **63**, 54 (1993).
[36] J. B. Theeten, D. E. Aspnes, F. Simondet, M. Erman, and P. C. Murau, J. Appl. Phys. **52**, 6788 (1981).
[37] T. Enomoto, R. Audo, H. Morita, and H. Nakayama, Jpn. J. Appl. Phys., Part 1 **17**, 1049 (1978).
[38] K. L. Luthra, J. Electrochem. Soc. **138**, 3001 (1991).